Enhancement of Doppler Resolution for Chirp-Sequence Modulated Radars

Fabian Roos*, Michael Barjenbruch†, Nils Appenrodt‡, Jürgen Dickmann‡, and Christian Waldschmidt*
*Institute of Microwave Engineering, Ulm University, 89081 Ulm, Germany
†Daimler AG, Trucks Advanced Engineering, 70546 Stuttgart, Germany
‡Daimler AG, Group Research and Advanced Engineering, 89081 Ulm, Germany
Email: fabian.roos@uni-ulm.de

***Abstract*—For automotive radar sensors the Doppler resolution is a key parameter, since it is used to separate targets which are in the same radial distance. For future applications the Doppler signature of targets can be exploited for classification purpose, e.g. discrimination among road users like pedestrians or bicyclists. In this paper, a signal processing scheme based on the chirp-sequence modulation principle is proposed to enhance the Doppler domain resolution. Simulations and measurement results are shown to prove the signal processing leading to an enhanced separability of close targets.**

I. Introduction

To enable driver assistance systems or autonomous driving the environment perception must be as precise as possible. Especially vulnerable road users like pedestrians need to be detected accurately for safety functions. In future, the Doppler distribution on extended targets can be exploited for classification. Those targets are often not distributed over a large radial distance and therefore the Doppler resolution is the only opportunity for classification [1]. In addition to classification, the Doppler resolution can be exploited to determine the velocity vector of moving extended targets as presented in [2]. For both applications numerous close targets in Doppler domain need to be distinguished.

An important parameter for radar sensors is the separability of close targets. Especially for the Doppler estimation the observation time is crucial. The longer the target is monitored, the more precise is the measurement. In addition, the peak width in spectrum is proportional to the observation time T_o of the time domain signal, because it can be interpreted as a multiplication with a rectangular function. In spectrum

$$\mathrm{rect}_{T_\mathrm{o}}(t) \quad \circ\!\!-\!\!\bullet \quad T_\mathrm{o}\frac{\sin(\pi f T_\mathrm{o})}{\pi f T_\mathrm{o}} \tag{1}$$

this corresponds to a convolution with a si function, and the first root is important for the peak width. A doubled observation time results in a halved peak width and hence a long measurement seems to be opportune. On contrast, a long observation time leads to a low update rate and therefore, a change in the environment is not fast enough detected.

This motivates the following presented approach to use signal processing to achieve an enhanced separability as well as a fast update rate. The observation time is not altered for fast updates, but for separability two consecutive measurements are evaluated together. For a chirp-sequence modulation format this results in the combination of two chirp blocks as depicted in Fig. 1. Between the two measured blocks time passed and the target moved with respect to its velocity. For a successful combination of two blocks this movement must be compensated. As will be shown, this requires an adjustment of both the frequency and the phase of the first measurement for every target.

This paper is organised as follows. In Section II the chirp-sequence modulation based block combination of two consecutive measurements is presented as well as a target selection which the new scheme is applied for. In Section III the simulative verification of the proposed signal processing is shown using the same parameters as the measurement results in Section IV.

II. Mathematical Model: Block Combination

In the next section a brief summary of the chirp-sequence modulation is given, on which the block combination in Section II-B is based. The block combination is only calculated for targets of interest. A possible selection principle of targets is introduced in Section II-C.

A. Chirp-Sequence Modulation

The proposed signal processing uses a chirp-sequence modulation, which uses short-time linear frequency ramps with chirp duration T_c and bandwidth B at the carrier frequency f_c. In [3] the intermediate frequency signal is derived for a target with constant velocity. One chirp-sequence block consists of L chirp ramps which are repeated every T_r. Written as a

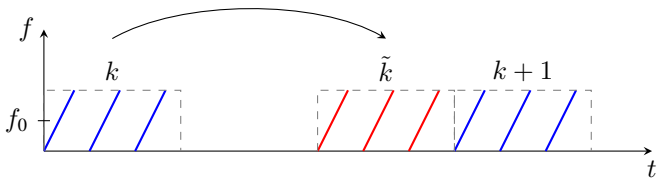

Fig. 1. Schematic for the proposed block combination evaluation of two consecutive chirp-sequence blocks. Block k is shifted and must be adapted.

complex signal with a window function $w(t)$ and an arbitrary amplitude A

$$s_{\mathrm{IF}}(t) = \sum_{l=0}^{L-1} w(t)\, A \cdot \mathrm{rect}\left(\frac{t - l\,T_\mathrm{r}}{T_\mathrm{c}}\right) \cdot \mathrm{e}^{\mathrm{i}2\pi\left[\frac{2f_\mathrm{c}(R+vT_\mathrm{r}l)}{c} + \left(\frac{2f_\mathrm{c}v}{c} + \frac{2B(R+vT_\mathrm{r}l)}{T_\mathrm{c}c}\right)t\right]}, \tag{2}$$

the intermediate frequency can be described. Due to the movement of the target between every ramp the distance is set up with $R + v\,T_\mathrm{r}\,l$. The range frequency f_R and velocity frequency f_v for Doppler determination

$$f_\mathrm{R} \approx \frac{2BR}{T_\mathrm{c}c}, \qquad f_\mathrm{v} = \frac{\mathrm{d}}{\mathrm{d}T_\mathrm{r}}\left(2\pi\frac{2f_\mathrm{c}(R + v\,T_\mathrm{r}\,l)}{c}\right) \tag{3}$$

are extracted by calculating a two-dimensional Fast Fourier Transform (*2D-FFT*) of $s_{\mathrm{IF}}(t)$. Applying this *FFT* to the samples of each chirp yields the range information. For each range cell of every ramp the second *FFT* results in the velocity information which is stored in the phase values of the samples.

B. Block Combination Evaluation

The resulting two-dimensional spectrum is analysed whereas peaks correspond to detected targets. Due to the passed time between two blocks the target moved with respect to its velocity. For the combination of two blocks this movement is corrected for. Therefore, first the radial movement must be compensated to prevent false distance extraction, second a continuous phase must be ensured for a correct Doppler information determination.

For each block the radial distance to the target is extracted using classic *2D-FFT* signal processing. Thus, the previous block k must be shifted by $\Delta R = R_{k+1} - R_k$ corresponding to a shift in frequency domain, as can be seen in (3). With the functional relationship

$$s_{\mathrm{IF}}(t) \cdot \mathrm{e}^{\mathrm{i}2\pi f_0 t} \quad \circ\!\!-\!\!\bullet \quad S_{\mathrm{IF}}(f - f_0) \tag{4}$$

this corresponds to a modulation in time domain with

$$\mathrm{e}^{\mathrm{i}2\pi\Delta f_\mathrm{R} t} = \mathrm{e}^{\mathrm{i}2\pi\frac{2B}{T_\mathrm{c}c}\Delta R\, t}. \tag{5}$$

The adaption of the phase in order to enable a correct Doppler frequency extraction is challenging. The accuracy of the extracted traveled distance is not sufficient to correct the phase by multiplying the block k with

$$\mathrm{e}^{\mathrm{i}\alpha} = \mathrm{e}^{\mathrm{i}2\pi\frac{2f_\mathrm{c}\Delta R}{c}} \tag{6}$$

to ensure a continuous phase trend between the blocks. This is due to the fact that even a slight error in ΔR, which is limited to the resolution of the range cells, results in a huge phase shift. Therefore the correct phase shift is estimated in the spectrum. The previous block k is modulated in frequency (5) and multiplied with different realisations of $\alpha \in [0°, 45°, \ldots, 315°]$ in (6). The previous and the actual

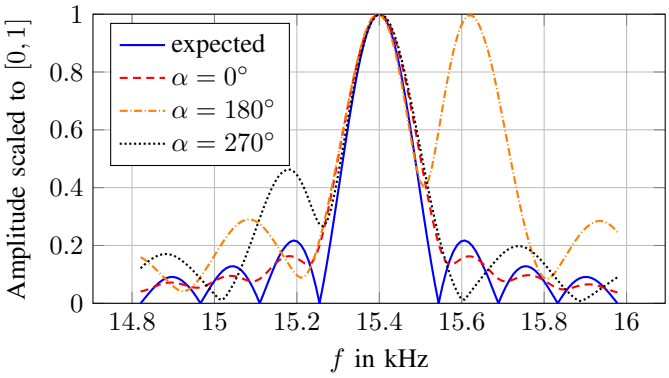

Fig. 2. Estimation of the phase shift between block $\tilde{k}$ and $k+1$ of Fig. 1. The desired spectrum (——) is compared in this example to an assumed phase shift of 0° (- - - -), 180° (-·-·-), and 270° (·····).

block are combined to a single measurement. Then the spectrum of the target peak around f_t in Doppler direction is compared to the positive part of the expected spectrum

$$\mathcal{F}^{+}\left\{\sin(2\pi f_\mathrm{t} t) \cdot \mathrm{rect}\left(\frac{t - T_\mathrm{o}}{2\,T_\mathrm{o}}\right)\right\} = -\frac{\mathrm{i}}{2} 2\,T_\mathrm{o}\,\mathrm{si}\left(\pi[f - f_\mathrm{t}]2\,T_\mathrm{o}\right) \cdot \mathrm{e}^{-\mathrm{i}2\pi(f - f_\mathrm{t})T_\mathrm{o}} \tag{7}$$

as in [4]. For each assumed phase shift α, the resulting spectrum is compared to the expected one as depicted in Fig. 2 for three different values of α. If the assumed phase shift is not correct this results in a deformed spectrum as for $\alpha = 180°$ or $\alpha = 270°$. For this simulation the actual value is $\alpha = 0°$. For comparison the absolute normalised expected and the absolute normalised actual spectrum are subtracted. The mean of the resulting value indicates how well the current assumed phase shift is.

To estimate the additional calculation costs the number of different realisations of α is important, because for every variation the previous chirp block matrix is modulated, phase shifted, and the spectrum is analysed for the expected range bin. For the optimal phase shift the chirp block matrix, consisting of the samples of the L ramps, twice as large as the classic one needs to be evaluated.

C. Target Selection

Due to the fact that usually every target has an unique radial velocity, the correction must be calculated independently for every target. This requires a pre-selection of targets of interest and a matching of targets in the previous and actual measurement.

Targets of interest are found using an ordered statistic-constant false alarm rate (*OS-CFAR*) algorithm [5]. The same target must be detected in the previous block k and the actual block $k+1$ for the block combination to work. Targets of interest are chosen considering the peak width in spectrum. A single target is narrower than two close targets in range and velocity. If the algorithm expects two close targets by judging the peak width, the block combination is performed for this target.

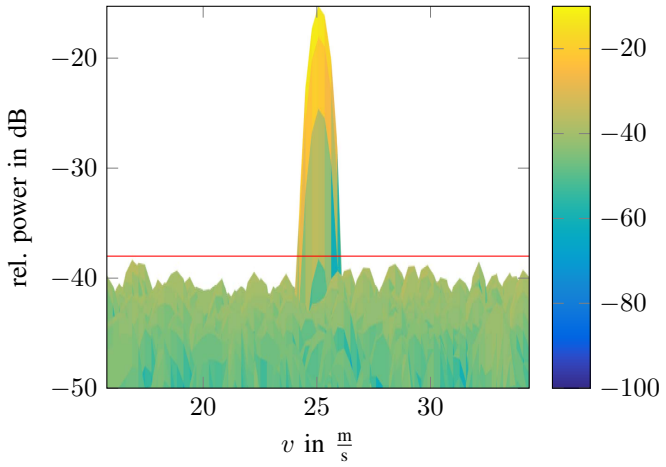

(a) The classic signal processing uses a *2D-FFT*.

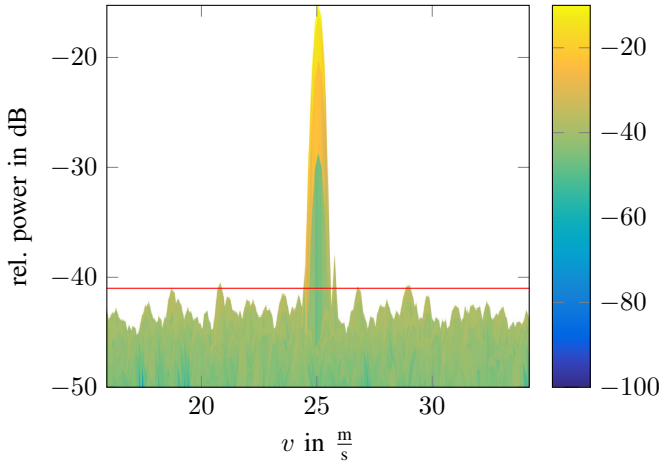

(b) Joint evaluation of the shifted and adapted chirp block $\tilde{k}$ with the consecutive block $k+1$ leading to a half wide peak and a lower noise floor.

Fig. 3. Simulation of a single target with a velocity of 25 $\frac{\text{m}}{\text{s}}$ using standard signal processing in (a) and the proposed block combination in (b). The noise floor (——) is in (b) 3 dB lower than in (a). Only part of the resulting spectrum is shown.

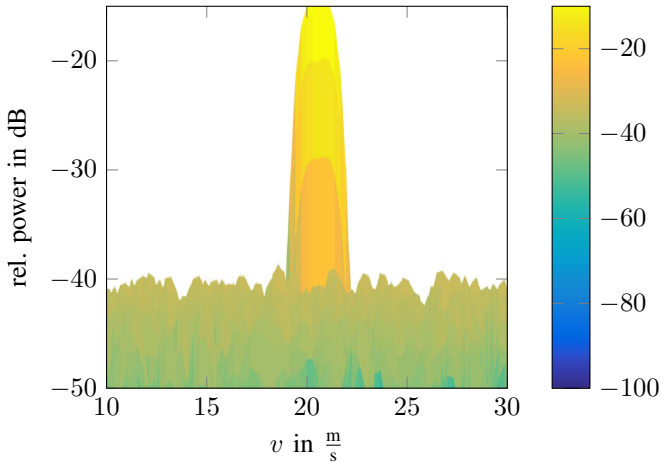

(a) The classic signal processing cannot separate two close targets.

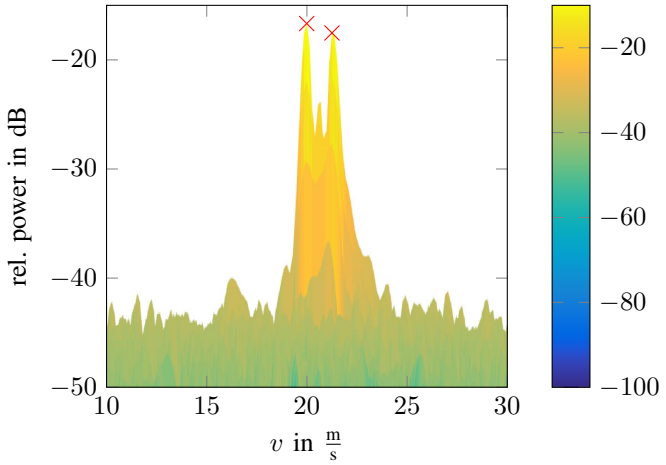

(b) Using the proposed block combination results in narrower peaks and enables the separation of the two targets.

Fig. 4. Simulation of two targets with the same radial distance but with a radial velocity of 20 $\frac{\text{m}}{\text{s}}$ and 21.1 $\frac{\text{m}}{\text{s}}$ using the standard signal processing in (a) and the proposed block combination in (b). Targets are detected (×) using the *OS-CFAR* algorithm. Only part of the resulting spectrum is shown.

III. Simulation Results

The block combination algorithm is verified using a simulation with various targets. The simulation environment replicates the measurement setup and uses therefore the same radar parameters which are listed in Tab. I. For a realistic simulation phase noise as described in [6] and implemented as in [7] is considered together with additive white Gaussian noise (*AWGN*). In Fig. 3 a target with a radial distance of 30 m with a radial velocity of 25 $\frac{\text{m}}{\text{s}}$ is simulated. The evaluation is done in (a) with a classic *2D-FFT* in contrast to the introduced block combination in (b). For both evaluations a zero padding to double the signal length is used together with a Hann window in range, velocity, and azimuth domain.

TABLE I
Specifications of Radar Parameters

Parameter	Value
carrier frequency f_c	77 GHz
bandwidth B	706 MHz
chirp duration T_c	20.480 µs
chirp repetition time T_r	27.015 µs
sampling frequency f_s	25 MHz
number of chirps L	128
window function	Hann
zero padding	signal length doubled

It can be seen that the peak width in velocity domain is halved in the block combination evaluation in contrast to the classic approach as expected from (1). The peak width is measured at the 3 dB point for each single target. In range direction, the width is unaffected by the block combination, because the observation time of one single frequency ramp is not altered.

If two targets at the same radial distance with slightly different radial velocities as in Fig. 4 are present, the peak

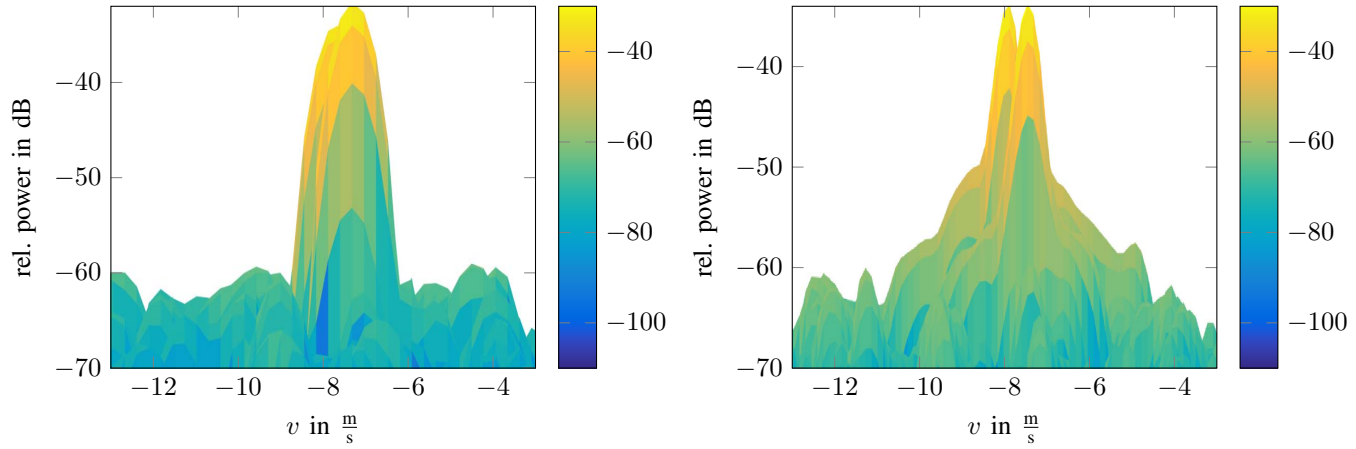

(a) The two corner reflectors cannot be distinguished.

(b) Only when using the block combination a separation is possible.

Fig. 6. In the analysed measurement (cf. Fig. 5) two close corner reflectors are present. With the standard signal processing in (a) the reflectors cannot be distinguished. This is only possible with block combination in (b). Only part of the resulting spectrum is shown.

width of the target in (a) is higher than expected for a single target. This indicates that the block combination should be applied, and as a result the two targets can be separated in (b).

Each sample has the same average noise power, but if twice as much samples are used to calculate the spectrum, the noise floor is lowered by 3 dB as can also be noticed in Fig. 3. But note that with the lowered noise the detection of weak targets is not improved by the block combination due to the fact that the targets must be known before the combination.

IV. Measurement Results

The block combination signal processing is validated with a measurement using a 77 GHz MIMO radar sensor which is mounted at the front of the vehicle. Two corner reflectors are placed on a traffic training centre, and the vehicle is driving with nearly constant velocity towards the two targets. Using the ten receive channels and a third *FFT* the radar image is generated. The evaluated measurement is shown in Fig. 5 together with a cutting of the video image showing the targets.

The cut through the range bins is shown in Fig. 6. Using the classic signal processing the two targets cannot be distinguished in (a), because the two peaks are merged together. Only with the knowledge that the peak is wider than a normal point target, it can be assumed that two targets are present. If the proposed block combination method is applied, the peaks are halved and can now be separated as shown in (b).

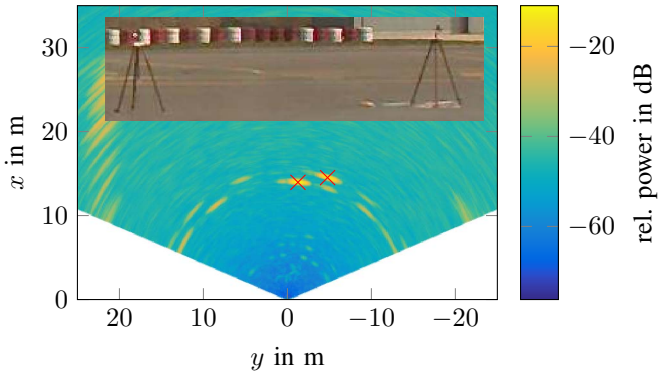

Fig. 5. Cartesian representation of the analysed measurement with two corner reflectors (×). The two targets are shown in the video image.

V. Conclusion

To achieve a high update rate the chirp-sequence modulation format is evaluated as known in literature. For selected targets the separability can be enhanced with the proposed block combination signal processing. Due to the halved target peaks in spectrum the resolvable minimal different Doppler velocity is reduced. The signal processing scheme is validated with different simulations and measurements using a 77 GHz MIMO radar sensor.

References

[1] E. Schubert, F. Meinl, M. Kunert, and W. Menzel, "High Resolution Automotive Radar Measurements of Vulnerable Road Users – Pedestrians & Cyclists," in *IEEE MTT-S International Conference on Microwaves for Intelligent Mobility (ICMIM)*, Apr. 2015, pp. 1–4.

[2] D. Kellner, M. Barjenbruch, K. Dietmayer, J. Klappstein, and J. Dickmann, "Instantaneous Lateral Velocity Estimation of a Vehicle using Doppler Radar," in *16th International Conference on Information Fusion*, Jul. 2013, pp. 877–884.

[3] V. Winkler, "Range Doppler Detection for automotive FMCW Radars," in *Proceedings of the 4th European Radar Conference (EuRAD)*, Oct. 2007, pp. 166–169.

[4] S. Olbrich and C. Waldschmidt, "New pre-estimation Algorithm for FMCW Radar Systems using the Matrix Pencil Method," in *European Radar Conference (EuRAD)*, Sep. 2015, pp. 177–180.

[5] H. Rohling, "Radar CFAR Thresholding in Clutter and Multiple Target Situations," *IEEE Transactions on Aerospace and Electronic Systems*, vol. AES-19, no. 4, pp. 608–621, Jul. 1983.

[6] A. Demir, A. Mehrotra, and J. Roychowdhury, "Phase Noise in Oscillators: A Unifying Theory and Numerical Methods for Characterization," *IEEE Transactions on Circuits and Systems I: Fundamental Theory and Applications*, vol. 47, no. 5, pp. 655–674, May 2000.

[7] A. Frischen, J. Hach, and C. Waldschmidt, "Performance Degradation in Cooperative Radar Sensor Systems due to Uncorrelated Phase Noise," in *Proceedings of the 11th European Radar Conference (EuRAD)*, Oct. 2014, pp. 241–244.